Proceedings of the 28th IEEE
EMBS Annual International Conference
New York City, USA, Aug 30-Sept 3, 2006

Automated Change Analysis From Fluorescein Angiograms for Monitoring Wet Macular Degeneration

Harihar Narasimha-Iyer, Ali Can, Badrinath Roysam and Jeffrey Stern

Abstract— **Detection and analysis of changes from retinal images is important in clinical practice, quantitative scoring of clinical trials, computer-assisted reading centers, and in medical research. This paper presents a fully-automated approach for robust detection and classification of changes in longitudinal time-series of Fluorescein Angiograms (FA). The changes of interest here are related to the development of Choroidal Neo-Vascularization (CNV) in Wet Macular Degeneration. Specifically, the changes in CNV regions as well as the Retinal Pigment Epithelium (RPE) hypertrophic regions are detected and analyzed to study the progression of disease and effect of treatment.**

Retinal features including the vasculature, vessel branching/crossover locations, optic disk and location of the fovea are first segmented automatically. The images are then registered to sub-pixel accuracy using a 12-dimensional mapping that accounts for the unknown retinal curvature and camera parameters. Spatial variations in illumination are removed using a surface fitting algorithm that exploits the segmentations of the various features. The changes are identified in the regions of interest and a Bayesian classifier is used to classify the changes into clinically significant classes. The automated change analysis algorithms were found to have a success rate of 83%.

I. INTRODUCTION

Macular degeneration is a broad term describing diseases that lead to a loss of central vision. Some of these diseases affect the macula directly, while Age related Macular Degeneration (AMD) affects the layer under the macula known as the Retinal Pigment Epithelium, or RPE [1]. There are two forms of macular degeneration namely dry (atrophic) macular degeneration and wet (neovascular/exudative) macular degeneration. Dry macular degeneration is the more common form of the disease and accounts for 90% of all AMD. Wet macular degeneration form is less common but more severe than the dry form. It accounts for approximately 10% of all AMD but 90% of all blindness from the disease. This form is characterized by Choroidal Neo-Vascularization (CNV), the development of abnormal blood vessels beneath the RPE layer of the retina. These vessels can bleed and eventually cause macular scarring which can result in profound loss of central vision(disciform scar).

Since the effect of drugs and treatments such as photodynamic therapy on CNV are still not well known, it is of interest to automatically monitor the changes and to extract quantitative measurements in these cases to study the effectiveness of the treatment and to track disease progression.

Figure 1 shows two FA images of the same eye captured one year apart. In the first image, the eye is starting to develop new choroidal vessels. In the second image, there is an increase in new vessels. The dark ring around the CNV is a thickening of the RPE layer believed to be the body's response to CNV and an attempt at containing the growth of new vessels. It is of interest to quantify how the new choroidal vessels (seen as the bright region in the FA), and the RPE ring (seen as the dark ring like structure), change over time.

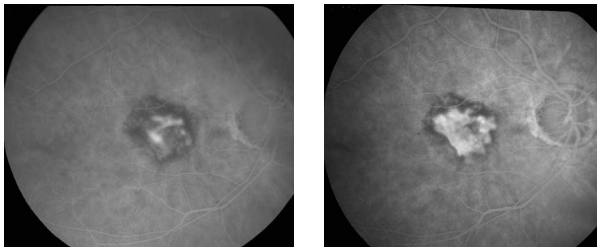

(a) (b)

Fig. 1. Fluorescein angiograms of an eye with wet macular degeneration. (a) Eye developing choroidal neovascularization (CNV) (b) Same eye as in (a) one year later. There is an increase in CNV between the two dates. Also, notice the dark ring around the CNV.

II. BACKGROUND

In an earlier paper [2], the authors had described an integrated framework for analyzing changes from color retinal fundus images. The main focus of that paper was robustly detecting and analyzing changes associated with diabetic retinopathy in the non-vascular regions. In this paper, we adapt the framework described in [2] to analyze changes from fluorescein angiograms. For completeness and clarity, we summarize the main elements of the change analysis framework described in [2].

A. Segmentation of Retinal Features

The retinal vasculature is first traced using an exploratory vessel tracing algorithm [3], [4]. This algorithm recursively finds connected pairs of parallel edges of blood vessels using directional edge templates. The branch points are extracted from the vessel centerlines as landmarks for registration. The optic disk is estimated using an adaptation of Hoover's fuzzy convergence algorithm [5], adaptive thresholding and template matching [2]. Based on the location of the optic disk, the fovea is detected using an adaptation of the algorithm described by Pinz et al. [6]. The optic disk detecion and fovea detection are performed on a color image that is registered to the FA image. This is because, the optic disk appears as a bright region in the color image and is much more distibguishable from the background in the color image compared to the FA image. Also, the registration algorithm to be described next, accurately registers between the FA

1-4244-0033-3/06/$20.00 ©2006 IEEE.

and color images and hence helps to map the positions of the features from the color image to the FA image precisely.

B. Sub-Pixel Accuracy Registration

We use the robust dual-bootstrap iterative closest point (ICP) algorithm [7] to register the images. This algorithm is feature based and uses the branching and cross-over points of the detected vasculature as landmarks to estimate a 12-dimensional spatial transformation between the images [8].

C. Robust Illumination Correction

Non-uniform illumination is a well known problem in retinal imaging and is primarily caused due to a combination of different factors. When comparing images taken at different times for changes, one must compensate for the spatially non-uniform illumination. In order to remove the effect of illumination, we use an algorithm that robustly estimates the illumination and reflectance components by homomorphic filtering and robust surface fitting, leveraging extracted retinal features [2]. The observed image is modeled as the product of an illumination component, $I(x, y)$, and a reflectance component, $R(x, y)$, in the following form:

$$F(x, y) = I(x, y)R(x, y). \tag{1}$$

Taking the logarithm of the observed image in equation 1, the slowly varying illumination field can be estimated by using a 4^{th} order polynomial surface [2]. i.e.

$$I(x, y) = exp(\mathbf{S}\vec{P}), \tag{2}$$

where $\mathbf{S}$ is a matrix composed of powers of x and y, the pixel locations and $\vec{P}$ is a vector of the polynomial coefficients. Using the estimated illumination component, the reflectance component can be recovered up to a scale factor as:

$$R(x, y) = exp(F_L(x, y) - \mathbf{S}\vec{P}). \tag{3}$$

where $F_L(x, y)$ is the logarithm of the observed image $F(x, y)$.

III. Identification of region of interest

In this study, we are specifically interested in the cases of choroidal neovascularization, where the RPE layer has formed a "ring"around the CNV. As mentioned before, this dark region is formed by a thickening of the RPE layer around the neovascularization. Inorder to analyze the changes inside the dark RPE region(which encloses the CNV), we need to identify the RPE region in each image. Candidate RPE regions are first obtained using a Gaussian mixture model formulation. This is followed by region growing to refine the region.

A. Obtaining Candidate Regions Using Mixture Modeling

The intensities in the FA image are modeled using a Gaussian mixture model. The probability of observing a pixel with intensity x is given by:

$$P(x) = \sum_{i=1}^{N} w_i p(x/g_i), \tag{4}$$

where w_i is the weight associated with component g_i and N is the number of components in the mixture model, which is set to 4 in our case. The likelihood of the pixel to have come from component g_i is given by:

$$p(x/g_i) = \frac{1}{\sqrt{2\pi\sigma_i^2}} exp\left(-\frac{(x-\mu_i)^2}{2\sigma_i^2}\right), \tag{5}$$

where μ_i and σ_i are the mean and standard deviation of g_i. The parameters of each of the components is estimated using the Expectation Maximization (EM) algorithm [11], [12].

The intensity distributions in FA images can vary significantly. In-order to capture these intensity variations, a two step approach is adopted. In the first step, the intensity of the background is identified by estimating the component parameters over the whole image and excluding the segmented vasculature and optic disk regions. Among the components in the Gaussian mixture, the background component is identified as follows. Intuitively, the background component should be the component with the maximum weight and least variance. Hence the components are sorted according to the ratio $\frac{w_i}{\sigma_i}$ and the component with the maximum value for this ratio is designated as the background component with mean μ_κ and standard deviation σ_κ. i.e,

$$\kappa = \underset{i=1,2,..N}{\arg\max}\{\frac{w_i}{\sigma_i}\}. \tag{6}$$

In the second step, the estimation is repeated over a small region centered around the fovea location. The location of the fovea can be detected from a color image that is registered to the FA image as described in section II. This region, to be referred to as the foveal region from now on, is a circular region with a diameter of 200 pixels centered around the fovea. The value of 200 was selected from the average size of the expected regions from the images under consideration. Once the parameters of the Gaussian components in the mixture model are estimated, we can identify the RPE hypertrophic region as described below.

Let R_r denote the dark RPE hypertrophic region. Component i is designated as belonging to R_r if its mean is sufficiently smaller than the average background intensity as shown:

$$\mu_i < \mu_\kappa - \alpha\sigma_\kappa. \tag{7}$$

α is a positive parameter that decides how much contrast is expected between the background and the dark region. α was set to 0.5 in this work.

The above step produces the initial segmentation for the RPE hypertrophic region.Since this initial segmentation is obtained inside the foveal region, and there is no guarantee that the desired region is fully segmented, a region growing algorithm is used to further refine the candidate region.

B. Refinement using Region Growing

Region growing is the process of joining neighboring pixels into larger regions based on common properties. Many different variations have been proposed for region growing [9], [10]. Here we use a version of the region growing

algorithm where a region is expanded based on the intensity properties of the neighboring pixels.

The set of boundary pixels for R_r is first identified. The regions adjoining the boundary pixels are then tested for a similarity criterion with the region under consideration. Suppose we are testing a small region y, which is adjacent to R_r. Then y is labeled as belonging to R_r if:

$$\frac{\mu_y - \mu_v}{\sigma_v} < 1, \tag{8}$$

where μ_y is the mean of the intensities in y, μ_v and σ_v are the mean and standard deviation of the intensities for pixels already in R_r. Equation (8) means that y is added to the current region if its average intensity is at the most one standard deviation greater than mean intensity of the initial region. The region growing step described above is iterated until convergence.

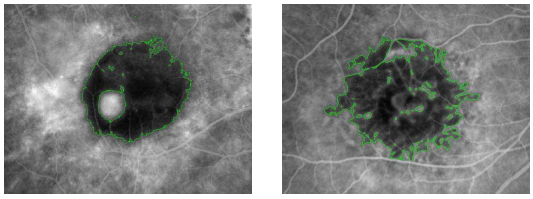

(a) (b)

Fig. 2. Sample segmentation results. The segmented RPE hypertrophic region is outlined in green.

Figure 2 shows sample segmentation results for two eyes. In order to find the region of interest for change analysis, a mask is found from the segmentation of the RPE region for each image. In cases where the RPE ring is well formed, the mask is the RPE segmentation with its interior filled in. In cases where the RPE ring is not well formed and has gaps, the mask is formed as the smallest polygon that inscribes the regions in the RPE segmentation. The logical OR of the masks from the two images is the region of interest for the change analysis. The next section describes how the changes are detected and classified.

IV. Bayesian Change Detection and Classification

Let the two fluorescein angiograms under consideration be denoted as $F_i(x, y)$ and $F_j(x, y)$. The reflectance components from each image,$R_i(x, y)$ and $R_j(x, y)$ are estimated as described in Section II. The difference image is formed as:

$$\triangle R(x, y) = R_i(x, y) - R_j(x, y). \tag{9}$$

The significant changes can now be detected from this difference image. Assuming a zero mean Gaussian distribution for the difference values, the change mask can be obtained by comparing the normalized sum square of the differences within a neighborhood as described by Aach et al.[13]:

$$\Omega_i = \frac{1}{\sigma_n^2} \Sigma_{(x,y)\epsilon w_i} (\triangle R(x, y))^2 \leq \Gamma, \tag{10}$$

where σ_n is the noise standard deviation of the difference in the no-change regions. The threshold Γ is derived from the fact that Ω follows a χ^2 distribution with N degrees of freedom, where N is the number of pixels in the window. Γ can be obtained for a particular false positive rate, α from the χ^2 tables. We use a 5×5 window ($N = 25$) and set $\alpha = 0.0005$.

Equation (10) is used to find the changes inside the region of interest. The change mask thus obtained is classified into different categories of change. To classify the change mask, each pixel in it needs to be described by some features. Our feature space consists of a two dimensional vector consisting of:

$$\begin{aligned} f_1 &= R_i(x, y), \\ f_2 &= R_j(x, y). \end{aligned} \tag{11}$$

A Bayesian classifier incorporating spatial contexual information is used to classify the pixels as desribed in [2]. The changes of interest in this application are the transitions from RPE to CNV, CNV to RPE and Normal to RPE. The change mask can be classified into these change classes. In order to make the change analysis robust to false change detection, the no-change classes, CNV to CNV, and RPE to RPE are also added to the set of classes mentioned above.

V. Experimental Results

A. Data Acquisition

The clinical data was recorded at Northeastern Retina Specialists (Albany, NY) using a Zeiss FF450 fundus camera and MRP Imaging System. Eyes with wet AMD, and exhibiting well defined RPE ring around the choroidal neovascularization were selected for the study. Fluorescein angiography was performed for each patient and during multiple visits to the clinic. Color images were also obtained prior to the FA examination. One frame from each FA series, collected at around one minute after dye injection were selected for further analysis. The frames were selected such that they had approximately the same brightness levels. This condition makes it possible to apply the robust illumination correction algorithm described in Section II.

A test set of 12 images from different subjects was used to evaluate the performance. Ground truth data was collected for each of the image by manually outlining the region of interest. This was done by an expert observer. The automatic change analysis results were then compared with the ground truth data.

TABLE I

Color codes used for displaying the change analysis results from FA images.

Type of Change	Display Color Code
RPE to CNV	
CNV to RPE	
Normal to RPE	
No change	N/A

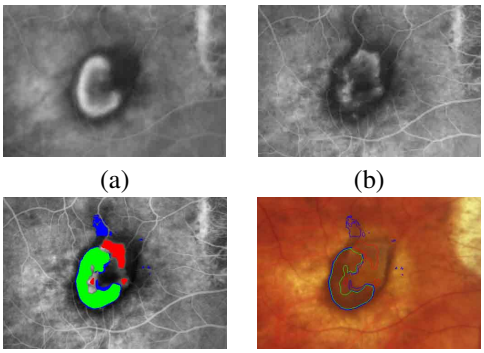

(a) (b) (c) (d)

Fig. 3. Sample change analysis results. (a) Eye with CNV, (b) After PDT treatment. (c) Color coded change analysis results. (d) The color coded change region boundaries superimposed on the corresponding color image.

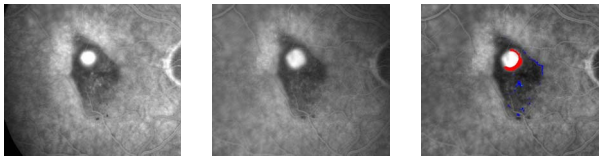

(a) (b) (c)

Fig. 4. Sample change analysis results (a) Eye with CNV, (b) Same eye after 17 days with no treatment (c) Color coded change analysis results.

B. Change Analysis Results

Figure 3 shows the automatically extracted changes for a patient who underwent Photo Dynamic Therapy (PDT) between the times the two images were taken. As expected, there was disappearance of CNV over some regions as well as appearance over other regions. In this case, the RPE hypertrophic layer was also seen to extend outwards a little. We are also able to relate the changes from the FA images to the color images. Figure 3d displays this capability, where change regions are overlaid on the corresponding color image. Figure 4 shows the change analysis results for another eye. The patient was treated with PDT two weeks before the first image was obtained. Figure 4 shows the change analysis between the first two images. The CNV increased between the two images. The RPE region also increased slightly.

The change classifications were compared to the different change regions derived from the manual segmentations. The change classification had a True Positive rate of 83% and a False Positive rate of 18%. The high false positive rate is due to the fact that the intensities of the CNV regions are highly variable and in some cases very close to the background intensity.

VI. CONCLUSIONS

The focus of this research was on developing software tools for higher-level, quantitative, and highly-automated change analysis from retinal images. Reliable, illumination-invariant, and fully-automated detection and analysis of changes in retinal images can form a valuable additional diagnostic resource for the clinician and researcher by mapping the dynamic nature of diseases. In this paper, we have extended the framework presented in [2] to analyze changes from Fluorescein Angiograms.

The automated change analysis techniques described in this paper have demonstrated to be effective on the patients considered till now. In order to draw biological conclusions about the changes and their patterns, we plan to do the analysis on a bigger sample population over an extended period of time.

REFERENCES

[1] F.L. Ferris 3rd, S.L Fine and L. Hyman, "Age-related macular degeneration and blindness due to neovascular maculopathy", *Archives of Opthalmology* , vol. 102, no. 11, 1984, pp 1640-1642.

[2] H. Narasimha-Iyer, A.Can, B.Roysam, C.V. Stewart, H. L. Tanenbaum, A. Majerovics and H. Singh, Automated Analysis of Longitudinal Changes in Color Retinal Fundus Images for Monitoring Diabetic Retinopathy, *IEEE Transactions on Biomedical Engineering* ,May 2005.

[3] A. Can, H. Shen, J. N. Turner, H. L. Tanenbaum and B. Roysam, "Rapid Automated Tracing and Feature Extraction From Live High-resolution Retinal Fundus Images Using Direct Exploratory Algorithms", *IEEE Transactions on Information Technology in BioMedicine*, vol. 3, no.2, June 1999, pp 125-138.

[4] K. H. Fritzsche, A. Can, H. Shen, C. Tsai, J. N. Turner, H. L. Tanenbaum, C.V. Stewart and B. Roysam, "Angiography and Plaque Imaging: Advanced Segmentation Methods. Chapter:Automated Model Based Segmentation, Tracing, and Analysis of Retinal Vasculature from Digital Fundus Images",CRC Press, Boca Raton.

[5] A. Hoover and M. Goldbaum, "Locating the optic nerve in a retinal image using the fuzzy convergence of the blood vessel", *IEEE Transactions on Meedical Imaging*, vol. 22, no. 8, 2003, pp 951-958.

[6] A. Pinz, S. Bernogger, P. Datlinger and A. Kruger, "Mapping the human retina", *IEEE Transactionss on Medical Imaging*, vol. 17, 1998, pp 606-619.

[7] C.V. Stewart, C.L. Tsai and B. Roysam, "The Dual-Bootstrap Iterative Closest Point algorithm with application to retinal image registration", *IEEE Transactions on Medical Imaging*, vol. 22, no. 11, 2003, pp 1379-1394.

[8] A. Can, C.V. Stewart, B. Roysam, and H.L. Tanenbaum, "A feature-based, robust, hierarchical algorithm for registering pairs of images of the curved human retina", *IEEE Transactions on Pattern Analysis and Machine Intelligence*, vol. 24, no.3, 2002, pp 347-363.

[9] R. Adams and L. Bischof, "Seeded region growing", *IEEE Transactions on Pattern Analysis and Machine Intelligence*, vol. 16, no.6, 1994, pp 641-647.

[10] S.-Y. Wan and W.E. Higgins, "Symmetric Region Growing", *IEEE Transactions on Image Processing*, vol. 12, no.9, 2003, pp 1007-1015.

[11] A. Dempster, N. Laird and D. Rubin,"Maximum likelihood from incomplete data via the EM algorithm", *Journal of the Royal Statistical Society* , vol. 39, 1977, pp 1-38.

[12] P. Paalanen, J.-K Kamarainen, J. Ilonen and H. Klviinen, "Feature Representation and Discrimination Based on Gaussian Mixture Model Probability Densities - Practices and Algorithms", Technical Report, Lappeenranta University of Technology, Department of Information Technology, 2005.

[13] T. Aach and A. Kaup,"Bayesian algorithms for adaptive change detection in image sequences using Markov Random Fields", *Signal Processing: Image Communication*, vol. 7, 1997, pp 147-160.